

Isospin-tracing: A probe of non-equilibrium in central heavy-ion collisions

F. Rami¹, Y. Leifels^{2,3}, B. de Schauenburg¹, A. Gobbi², B. Hong⁴, J.P. Alard⁵, A. Andronic⁶, R. Averbeck², V. Barret⁵, Z. Basrak⁷, N. Bastid⁵, I. Belyaev⁸, A. Bendarag⁵, G. Berek⁹, R. Čaplar⁷, N. Cindro⁷, P. Crochet⁵, A. Devismes², P. Dupieux⁵, M. Dželalija⁷, M. Eskef³, C. Finck², Z. Fodor⁹, H. Folger², L. Fraysse⁵, A. Genoux-Lubain⁵, Y. Grigorian², Y. Grishkin⁸, N. Herrmann^{2,3}, K.D. Hildenbrand², J. Kecskemeti⁹, Y.J. Kim⁴, P. Koczon², M. Kirejczyk¹⁰, M. Korolija⁷, R. Kotte¹¹, M. Kowalczyk¹⁰, T. Kress², R. Kutsche², A. Lebedev⁸, K.S. Lee⁴, V. Manko¹², H. Merlitz³, S. Mohren³, D. Moisa⁶, J. Mösner¹¹, W. Neubert¹¹, A. Nianine¹², D. Pelte³, M. Petrovici⁶, C. Pinkenburg², C. Plettner¹¹, W. Reisdorf², J. Ritman², D. Schüll², Z. Seres⁹, B. Sikora¹⁰, K.S. Sim⁴, V. Simion⁶, K. Siwek-Wilczyńska¹⁰, A. Somov⁸, M.R. Stockmeier³, G. Stoica⁶, M. Vasiliev¹², P. Wagner¹, K. Wiśniewski², D. Wohlfarth¹¹, J.T. Yang⁴, I. Yushmanov¹², A. Zhilin⁸

the FOPI Collaboration

¹ Institut de Recherches Subatomiques, IN2P3-CNRS, Université Louis Pasteur, Strasbourg, France

² Gesellschaft für Schwerionenforschung, Darmstadt, Germany

³ Physikalisches Institut der Universität Heidelberg, Heidelberg, Germany

⁴ Korea University, Seoul, South Korea

⁵ Laboratoire de Physique Corpusculaire, IN2P3/CNRS, and Université Blaise Pascal, Clermont-Ferrand, France

⁶ National Institute for Nuclear Physics and Engineering, Bucharest, Romania

⁷ Rudjer Boskovic Institute, Zagreb, Croatia

⁸ Institute for Theoretical and Experimental Physics, Moscow, Russia

⁹ Central Research Institute for Physics, Budapest, Hungary

¹⁰ Institute of Experimental Physics, Warsaw University, Poland

¹¹ Forschungszentrum Rossendorf, Dresden, Germany

¹² Kurchatov Institute, Moscow, Russia

Four different combinations of $^{96}_{44}\text{Ru}$ and $^{96}_{40}\text{Zr}$ nuclei, both as projectile and target, were investigated at the same bombarding energy of 400A MeV using a 4π detector. The degree of isospin mixing between projectile and target nucleons is mapped across a large portion of the phase space using two different isospin-tracer observables, the number of measured protons and the $t/3\text{He}$ yield ratio. The experimental results show that the global equilibrium is not reached even in the most central collisions. Quantitative measures of stopping and mixing are extracted from the data. They are found to exhibit a quite strong sensitivity to the in-medium (n,n) cross section used in microscopic transport calculations.

PACS numbers: 25.75.-q; 25.75.Dw; 25.75.Ld

Central heavy-ion collisions represent a valuable tool for studies of hot and dense nuclear matter where one hopes to infer valuable information on the nuclear equation of state (EOS) and on modifications of hadrons in the nuclear medium. While fluid dynamics calculations offer the most direct way to extract the EOS from the observed data [1], it is still an open question whether the widely applied, at least local, equilibrium assumption is valid in such reactions, or whether significant non-equilibrium effects rather require the application of more elaborated microscopic transport models [2–4]. The issue of equilibration is expected to be influenced by in-medium effects (such as Pauli blocking, Fermi motion) on the 'hard' scattering processes, by early 'soft' deflections in the momentum-dependent mean fields, and by

finite-size (corona) effects.

Experimental observations of non-equilibrium were concentrated, up to now, on the measurement of the momentum distribution of the products emerging from a mid-rapidity "source" of symmetric colliding systems. Observables of interest were the width of rapidity distributions [3,5] or the overall shape of the source [6,7]. The sensitivity of such observables is however reduced by effects like rescattering during the late phase of expansion.

In order to improve on the sensitivity we have designed a new type of measurement which makes use of the isospin (N/Z) degree of freedom in combination with a new high precision experimental method. As it will be shown in some details later, (N/Z) can be used as a tracer in order to attribute the measured nucleons (on average) either to the target or to the projectile nucleons. It is therefore possible to extract rapidity-density distributions separately for projectile and target nucleons. This gives access to new more sensitive observables, like stopping and mixing, of the early equilibration process.

The experiment was carried-out using reactions between equal mass nuclei $A = 96$, at an incident energy of 400A MeV. Isotopes of Ru and Zr were taken as projectile and target making use of all the four combinations: Ru+Ru, Ru+Zr, Zr+Ru and Zr+Zr. This choice of isotopes takes advantage of an almost unique possibility offered by the periodic table of stable isotopes, while searching for two isobars of the largest possible N/Z difference (the N/Z ratio is equal to 1.18 and 1.40 for $^{96}_{44}\text{Ru}$ and $^{96}_{40}\text{Zr}$, respectively) which can be used both as pro-

jectile and target. The bombarding energy was chosen at the minimum of the (n,n) cross section where the relative motion is significantly larger than the Fermi motion, but sufficiently low to avoid inelastic (n,n) channels, while the (n,n) angular distribution is almost isotropic.

The experiment was performed at SIS/ESR-Darmstadt using the FOPI apparatus [8,9]. The products of interest here, p, d, t and ^3He were identified: i) forward at laboratory angles $1.2^\circ < \theta_{\text{lab}} < 30^\circ$ using the TOF-wall and the HELITRON drift chamber and ii) backwards ($34^\circ < \theta_{\text{lab}} < 145^\circ$) using the Central Drift Chamber (CDC). About 66% of the total charge emitted in the backward center-of-mass (c.m.) hemisphere was detected by the CDC. Protons, deuterons and tritons constitute a large fraction of the emitted charge, about 40%, 30% and 10%, respectively.

Central collisions were selected requiring a large ratio of total transverse to total longitudinal energy, E_{RAT} [6,7]. E_{RAT} is determined event wise by including all detected particles: $E_{\text{RAT}} = \sum_{i=1}^M E_t^i / \sum_{i=1}^M E_l^i$, where E_t^i and E_l^i are the transverse and longitudinal energies of the particle i and M is the number of detected particles. The $E_{\text{RAT}} > 1.4$ cut used here corresponds to about 1.5% of the total reaction cross section and to a geometrical impact parameter $b_{\text{geom}} \leq 1.3$ fm in a sharp-cut-off approximation.

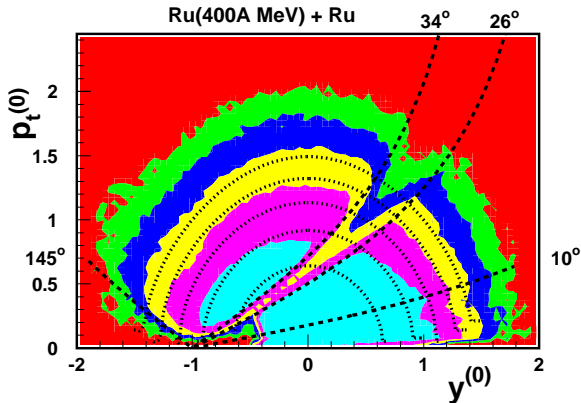


FIG. 1. Invariant cross section in the $(y^{(0)}, p_t^{(0)})$ plane of $Z = 1$ particles measured in the CDC and the TOF-wall, under the $E_{\text{RAT}} > 1.4$ centrality cut. $y^{(0)}$ is the normalized rapidity, i.e. the particle c.m. rapidity divided by the projectile rapidity in the c.m. system. $p_t^{(0)}$ denotes the normalized transverse momentum, i.e. the particle transverse momentum per nucleon divided by the c.m. projectile momentum per nucleon. The grey levels correspond to different logarithmic cuts in the invariant cross section. The dashed lines show the acceptance of the CDC ($34^\circ < \theta_{\text{lab}} < 145^\circ$) and the HELITRON ($10^\circ < \theta_{\text{lab}} < 26^\circ$) detector components. The circles correspond to constant c.m. energies per nucleon: from the inner to the outer, 40, 80, 120, 160 and 200A MeV.

Fig. 1 shows that the events selected under the $E_{\text{RAT}} > 1.4$ condition exhibit, in a representation of rapidity versus transverse momentum, a nearly isotropic

source for the observed hydrogen ($Z = 1$) products. This is in agreement with previous observations [5–7,10].

The (N/Z) -tracer method is based on the following idea: let us assume that we are observing the final number of protons, Z in a given cell of the momentum space. The expected yield Z^{Ru} measured for the Ru+Ru reaction is higher than Z^{Zr} of the Zr+Zr reaction since Ru has 44 protons as opposed to 40 for Zr. Such measurements using identical projectile and target deliver calibration values Z^{Ru} and Z^{Zr} for each observed cell. In the case of a mixed reaction, Ru+Zr or Zr+Ru, the measured proton yield Z takes values intermediate between the calibration values (Z^{Ru} , Z^{Zr}). If e.g. Z is close to Z^{Ru} in a Ru+Zr reaction, means that the cell is populated predominantly from nucleons of the Ru-projectile while if it is close to Z^{Zr} it is mostly populated from nucleons of the Zr-target. In this way it is possible to trace back the relative abundance of target to projectile nucleons contributing to a given cell. If the mixed value Z varies linearly between the two extremes of the calibration values (Z^{Ru} , Z^{Zr}) as a function of the relative abundance of target versus projectile nucleons, such an abundance can be most easily derived. As it will be shown this is indeed the case for protons but it is not the case if we use as a (N/Z) -tracer variable not the number of protons but e.g. the relative tritium to ^3He abundance in the cell. The t/ ^3He -ratio varies non-linearly between the two extreme of the calibration reactions, but this can be taken into account and, as it will be shown, consistent results are obtained with different (N/Z) -tracer variables.

The following definition for the relative abundance of the projectile-target nucleons has been adopted:

$$R_Z = \frac{2 \times Z - Z^{\text{Zr}} - Z^{\text{Ru}}}{Z^{\text{Zr}} - Z^{\text{Ru}}} \quad (1)$$

where R_Z takes $+1$ for Zr+Zr and -1 for Ru+Ru. In the case of full equilibrium in a mixed reaction, R_Z would be equal to 0 everywhere independently of the location of the cell (for the case of a linear dependence of Z).

Several important advantages of the method can be mentioned: (i) the four reaction combinations are investigated, under identical experimental conditions so that the ratios are insensitive to systematic uncertainties due to the apparatus. The errors are essentially of statistical nature and profit from the high yield in the considered cell. (ii) the mixed reaction Zr+Ru is the same as Ru+Zr except that target and projectile are inverted: this allows forward-backward cross-checks of the apparatus which in addition can also be obtained from the symmetric Ru+Ru and Zr+Zr reactions. (iii) using the four reactions the full information needed can be obtained by measuring only within the c.m. backward or only the c.m. forward hemisphere. A measurement of both hemispheres is redundant. The (N/Z) -variable was used at low bombarding energies [11–13] but without taking ad-

vantage, like here, of four target/projectile combinations with their symmetries and redundancies.

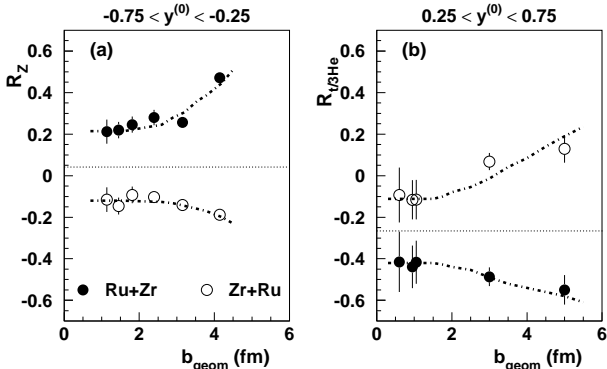


FIG. 2. Two isospin-tracer observables as a function of the geometrical impact parameter: R_Z (panel a) and $R_{t/3\text{He}}$ (panel b). They are determined in the c.m. rapidity range $-0.75 \leq y^{(0)} \leq -0.25$ and $0.25 \leq y^{(0)} \leq 0.75$, respectively. The horizontal dotted lines correspond to the values ($R_Z = 0.04$ and $R_{t/3\text{He}} = -0.27$) at halfway between the Ru+Zr and Zr+Ru experimental points in the $b_{\text{geom}} \leq 1.5$ fm region. The dotted-dashed lines are just to guide the eye.

The results to be presented here concentrate on two tracer-observables: (A) the sum (Z) of the number of detected free protons plus the number of protons detected within the deuterons. (B) the relative abundance of tritium to ^3He ($t/^3\text{He}$). Observable (A) was measured in the backward c.m. hemisphere using the CDC: this has the advantage to minimize background originating from the oxygen content of the (ZrO_2) target. Observable (B) was measured in the forward c.m. hemisphere using HELITRON and TOF-wall profiting from a good time-of-flight particle identification.

Results on the centrality dependence of the abundance ratios are presented in Fig. 2. The selected momentum cell is rather wide and integrates over a large rapidity bin. Panels (a) and (b) show results obtained from, proton yields and $t/^3\text{He}$ -ratios, respectively. The quantity $R_{t/3\text{He}}$ is defined in a similar way as for R_Z , using equation (1) with Z being replaced by the $t/^3\text{He}$ abundance ratio. The impact parameter b_{geom} is derived by integrating over the measured cross section as a function of E_{RAT} or of the charged particle multiplicity. Except for an off-set of $R_{t/3\text{He}} = -0.27 \pm 0.07$ for the $t/^3\text{He}$ -ratio, both figures display the same trends. Such an off-set can be understood from a non-linear dependence of the $t/^3\text{He}$ ratio as a function of isospin. We find that a dependence more than quadratic like $t/^3\text{He} = 1 + \text{const} \times \left(\frac{N-Z}{N+Z}\right)^{2.5}$ satisfies the measured off-set and agrees with known experimental systematics [14]. The off-set on Fig. 2a is very small (0.04 ± 0.03) and demonstrates the linear dependence of variable (A), what is also confirmed in Fig. 3a: at mid-rapidity ($y^{(0)} = 0$) the ratio R_Z is very close to 0, for both mixed reactions as expected from symmetry.

The results of Fig. 2 are consistent with the picture of an incomplete global equilibrium which persists up to the end of the collision, an observation that holds even for the most central collisions, for $b_{\text{geom}} \rightarrow 0$.

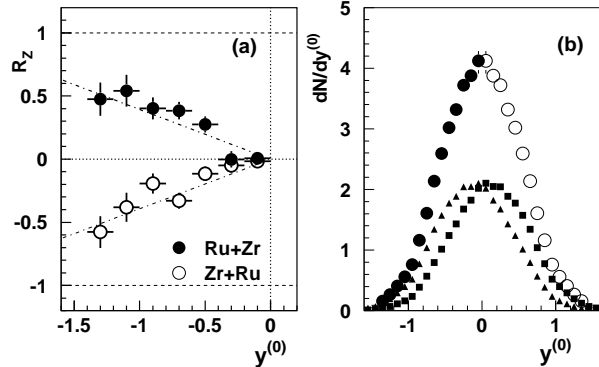


FIG. 3. Panel (a) shows the tracer observable R_Z as a function of the normalized c.m. rapidity for central collisions. The experimental results are shown for both isospin asymmetric reactions Ru+Zr (full circles) and Zr+Ru (open circles). The error bars correspond to statistical uncertainties. The horizontal dashed lines indicate the values of $R_Z = +1$ and -1 corresponding to the isospin symmetric reactions Zr+Zr and Ru+Ru, respectively. Panel (b) displays the experimental c.m. rapidity distribution (circles) of protons, free plus those detected within the deuterons, in central Ru+Ru collisions. Data points in the backward hemisphere (full circles) were obtained from the CDC detector. Those in the forward region (open circles) were obtained by assuming a backward/forward symmetry. The two other distributions have been obtained by unfolding the overall distribution into 'projectile' (squares) and 'target' (triangles) components.

After the inspection of the centrality dependence of Fig. 2, we show in Fig. 3 the rapidity dependence of R_Z for the most central collisions. For this purpose we use the proton yield (A) whose relatively high cross sections permit a fine subdivision of the rapidity bins. Inverting projectile and target changes, as expected, the sign of the R_Z -values; besides that, both results agree within errors. The dashed-dotted line ($\pm 0.393 y^{(0)}$) describes an average of both measurements (being the same except for the sign) and can be used to deconvolute the overall measured rapidity distribution $dN/dy^{(0)}$ (Fig. 3b) for Ru+Ru into *separated rapidity distributions for the projectile- and for the target-nucleons*. For each rapidity bin, the number of projectile (target) nucleons was obtained as $N_{\text{pr}} = 0.5 (1 + 0.393 y^{(0)}) N$ ($N_{\text{tr}} = 0.5 (1 - 0.393 y^{(0)}) N$). The overall $dN/dy^{(0)}$ distribution was obtained by extrapolating the measured transverse momentum spectra, within the backward detector acceptance, according to the procedure described in [5]. After deconvolution a shift between the two deduced rapidity distributions emerges, demonstrating that a memory of the initial target/projectile translatory motion survives throughout a central collision.

The separated projectile (or target) rapidity distribution can be readily parametrized into: (i) a shift $\langle y_{\text{pr}}^{(0)} \rangle$ of the mean value with respect to mid-rapidity; $\langle y_{\text{pr}}^{(0)} \rangle = 0$ corresponds to full stopping and full thermo/chemical equilibrium, while $\langle y_{\text{pr}}^{(0)} \rangle = 1$ corresponds to the initial projectile rapidity without any stopping; positive values of $\langle y_{\text{pr}}^{(0)} \rangle$ are expected for transparency, negative values for a backward rebound of the projectile nucleons from the target. (ii) a mixing value $M_{\text{pr}} = (N_f - N_b)/(N_f + N_b)$, where N_f is the number of projectile nucleons emitted forward and N_b backwards; M_{pr} is a measure of non-equilibrium effects. (iii) a width of the unfolded distribution, σ_{pr} .

TABLE I. Mean value $\langle y_{\text{pr}}^{(0)} \rangle$, width σ_{pr} of the projectile rapidity distribution (in $y^{(0)}$ units) and mixing observable M_{pr} (see text) obtained for Ru+Ru. (1): values extracted from the data; systematic errors on $\langle y_{\text{pr}}^{(0)} \rangle$ and M_{pr} are about 10%. (2): IQMD predictions obtained by applying the (N/Z) -tracer method. (3): same as (2) but using the detector filter. (4): same as (2) but here IQMD predictions are obtained by tagging projectile and target nucleons in the model. (5): same as (4) with $\sigma_{\text{nn}}^{\text{med}} = 0.5 \sigma_{\text{nn}}^{\text{free}}$. (6): same as (4) with $\sigma_{\text{nn}}^{\text{med}} = 1.2 \sigma_{\text{nn}}^{\text{free}}$. (7): same as (4) but without MDI.

	(1)	(2)	(3)	(4)	(5)	(6)	(7)
$\langle y_{\text{pr}}^{(0)} \rangle$	0.11	0.15	0.15	0.16	0.33	0.11	0.10
σ_{pr}	0.52	0.55	0.56	0.55	0.59	0.54	0.52
M_{pr}	0.17	0.22	0.21	0.23	0.43	0.16	0.15

The defined values are well suited in order to characterize with few numbers the separated distributions and the strength of the non-equilibrium effects. They are useful in order to verify with the help of theoretical models [15–17] the relevance of the (N/Z) -tracer method and effects due to the experimental filter. Such studies have been performed here in the context of the IQMD-model [15]. Calculations were done using a stiff ($K = 380$ MeV) EOS and momentum dependent interactions (MDI) for impact parameter selections similar to those applied to the data. The results (Table I) show that the extracted values are reliable. As shown from the IQMD calculations, the effect of the detector filter is negligible. This is due to the fact that the method relies on relative quantities. The systematic errors ($\sim 10\%$) on the experimental $\langle y_{\text{pr}}^{(0)} \rangle$ and M_{pr} values take into account the influence of other particle species (t, α and heavier fragments) not considered in the analysis. It is interesting to note also in Table I that the values obtained by applying the (N/Z) -tracer method to the IQMD events are very close to those extracted by tagging the projectile and target nucleons in the model. This confirms the validity of the (N/Z) -tracer method proposed in this Letter. The dependence of the extracted parameters on the in-medium (n,n) -cross section, $\sigma_{\text{nn}}^{\text{med}}$, is shown in Table I. Both ob-

servables $\langle y_{\text{pr}}^{(0)} \rangle$ and M_{pr} exhibit a quite strong sensitivity to $\sigma_{\text{nn}}^{\text{med}}$ and depend also on MDI effects. On the other hand, the influence of the stiffness of the EOS was found to be very weak. A comparison to the experiment leads to a value of $\sigma_{\text{nn}}^{\text{med}}$ slightly higher (by about 20%) than the free (n,n) -cross section, $\sigma_{\text{nn}}^{\text{free}}$: a significant reduction of $\sigma_{\text{nn}}^{\text{med}}$ seems to be excluded within this model.

In conclusion, the proposed experiment and method demonstrate a high sensitivity to non-equilibrium effects, which are found to persist up to the end of a reaction even in the most central collisions. This confirms the necessity to use non-equilibrium dynamical calculations for studies of in-medium effects and of the EOS of high density nuclear matter.

This work was supported in part by the French-German agreement between GSI and IN2P3/CEA, by the PROCOPE-Program of the DAAD and by the Korea Research Foundation (Contract No. 1997-001-D00117). The BMBF has funded the collaboration under the contracts RUM-005-95 and POL-119-95. The DFG has given support in the framework of the projects 436 RUS-113/143/2 and 446 KOR-113/76/0. One of us (Y.L.) would also like to acknowledge support from the Margarete-von-Wrangell-Program.

- [1] H. Stöcker and W. Greiner, Phys. Rep. **137** (1986) 277.
- [2] G. F. Bertsch, H. Kruse and S. Das Gupta, Phys. Rev. **C 32** (1984) R673.
- [3] J. Aichelin, Phys. Rep. **202** (1991) 233.
- [4] H. Feldmeier, Nucl. Phys. **A 515** (1990) 147.
- [5] B. Hong *et al.*, FOPI Collaboration, Phys. Rev. **C 57** (1998) 244.
- [6] S. C. Jeong *et al.*, FOPI Collaboration, Phys. Rev. Lett. **72** (1994) 3468.
- [7] W. Reisdorf *et al.*, FOPI Collaboration, Nucl. Phys. **A 612** (1997) 493.
- [8] A. Gobbi *et al.*, FOPI Collaboration, Nucl. Inst. Meth. **A 324** (1993) 156.
- [9] J. Ritman *et al.*, FOPI Collaboration, Nucl. Phys. (Proc. Suppl.) **B 44** (1995) 708.
- [10] M. A. Lisa, EOS Collaboration, Phys. Rev. Lett. **75** (1995) 2662.
- [11] S. J. Yennello *et al.*, Phys. Lett. **B 321** (1994) 15.
- [12] H. Johnston *et al.*, Phys. Lett. **B 371** (1996) 186.
- [13] H. Johnston *et al.*, Phys. Rev. **C 56** (1997) 1972.
- [14] S. Nagamiya *et al.*, Phys. Rev. **C 24** (1981) 971.
- [15] C. Hartnack *et al.*, Eur. Phys. J. **A 1**, (1998) 151.
- [16] S. A. Bass *et al.*, Prog. Part. Nucl. Phys. **41** (1998) 225.
- [17] A. Hombach, W. Cassing and U. Mosel, Eur. Phys. J. **A 5**, (1999) 77.